ADVANCED ENERGY MATERIALS
www.advenergymat.de

Domain Wall Free Polar Structure Enhanced Photodegradation Activity in Nanoscale Ferroelectric $Ba_xSr_{1-x}TiO_3$

Yaqiong Wang, Man Zhang, Jianguo Liu, Haibin Zhang, Feng Li, Chiao-Wei Tseng, Bin Yang, Graham Smith, Jiwei Zhai, Zhen Zhang, Steve Dunn, and Haixue Yan**

Ferroelectric materials exhibit anomalous behavior due to the presence of domains and domain walls which are related to the spontaneous polarization inherent in the crystal structure. Control of ferroelectric domains and domain walls has been used to enhance device performances in ultrasound, pyroelectric detectors, and photovoltaic systems with renewed interest in nanostructuring for energy applications. It is also known that ferroelectrics including domain walls can double photocatalytic rate and increase carrier lifetime from microsecond to millisecond. However, there remains a lack of understanding on the different contributions of the domain and domain walls to photocatalytic activities. Herein it is found, by comparing samples of nanostructured $Ba_xSr_{1-x}TiO_3$ with and without a polar domain, that the material with polar domains has a faster reaction rate ($k = 0.18$ min^{-1}) than the nonpolar one ($k = 0.11$ min^{-1}). It is further revealed that the observed enhanced photoactivity of perovskite ferroelectric materials stems from the inherent polarization of the domain instead of domain walls. Here, the new understanding of the underlying physics of materials with a spontaneous dipole opens a door to enhance the performance of light induced energy harvesting systems.

1. Introduction

Questions arising from the fundamental physics related to domain stability have been evident for ferroelectric materials since ferroelectric domains were first reported.[1,2] This interest extends to the aspects of domain wall motion, influence of domain on charge separation, and the interactions of dipoles as the domain size approaches nanoscale and ultimately the unit cell. Computational studies performed on the surfaces restructuring of ferroelectric during a phase change show the advantages of using polar materials to drive surface chemical reactions over a polydomain material.[3] To date experimental and computational studies have mainly focused on polycrystalline, or polydomain ferroelectric single crystals. These studies have largely shown that the ferroelectric material can enhance photocatalytic activity and energy conversion efficiency

Dr. Y. Wang, M. Zhang, Dr. H. Yan
School of Engineering and Materials Science
Queen Mary University of London
Mile End Road, London E1 4NS, UK
E-mail: h.x.yan@qmul.ac.uk

Dr. Y. Wang, Prof. S. Dunn
School of Engineering
London South Bank University
103 Borough Road, London SE1 0AA, UK
E-mail: dunns4@lsbu.ac.uk

Prof. J. Liu
School of Environment
Tsinghua University
1 Qinghuayuan, Beijing 100084, China

The ORCID identification number(s) for the author(s) of this article can be found under https://doi.org/10.1002/aenm.202001802.

DOI: 10.1002/aenm.202001802

Prof. H. Zhang
Innovation Research Team for Advanced Ceramics, Institute of Nuclear Physics and Chemistry
China Academy of Engineering Physics
Mianyang 621900, China

Dr. F. Li, Prof. J. Zhai
Key Laboratory of Advanced Civil Engineering Materials of Ministry of Education, Functional Materials Research Laboratory, School of Materials Science and Engineering
Tongji University
4800 Caoan Road, Shanghai 201804, China

Dr. C.-W. Tseng, Prof. Z. Zhang
Division of Solid-State Electronics, Department of Electrical Engineering
Uppsala University
Lagerhyddsvagen 1, Uppsala, Sweden

Dr. B. Yang, Prof. G. Smith
Faculty of Science and Engineering
University of Chester
Thornton Science Park, Chester CH2 4NU, UK

in photovoltaic devices.[4] The development of organic halide perovskites as sensitizers in photovoltaic devices has brought the concept of enhanced photo-carrier separation effect into sharp focus for polydomain polar materials.[5] The growing evidence of polar nanodomains in lead halide systems further confirms the inherent influence of polar materials in light harvesting.[6] The studies conducted on metal halide systems is also supported by previous work on metal oxide materials showing enhanced photon induced performance.[7] Despite these studies, a fundamental question still remains to be answered: are these ferroelectric enhanced device performance resulted from the domain wall, or from the inherent spontaneous polarization in the domains of the ferroelectric material.

Domain walls have significant influence on the local surface potential and surface free energy[8,9] and may influence the surface chemistry in an analogous manner to the anomalous photocatalytic field.[10] When assessing photovoltaic and photocatalytic performance of polar materials the contribution from both domain and domain walls should be considered. Atomic level structures of domain wall were successfully characterized using advanced aberration-corrected transmission electron microscope (STEM) in some ferroelectrics, which shows that the polarization in domain walls is smaller than that in domains.[11] Furthermore, complications also arise to understand the domain structure in nanostructured systems. Tools such as X-ray diffraction (XRD) can give useful insights but XRD is typically inferring the polar/nonpolar structure of materials from the unit cell by characterizing their crystallography. It often fails on nanosized ferroelectrics due to the lack of long-range coherency of distortions.[12,13] Techniques such as transmission electron microscopy (TEM), piezo-force microscopy (PFM), and Raman, have proved the existence of spontaneous polarization in ferroelectric particles at the unit cell scale.[14] These complications in interpreting analytical data make it difficult to fully understand the domain structure of small ferroelectric systems, and therefore any influence on the behavior of photo-induced carriers.

In order to investigate whether domain walls are the dominant cause of the enhanced carrier separation as well the associated photocatalytic performance improvement, two single-crystalline $Ba_xSr_{1-x}TiO_3$ (BST) nanoparticles were prepared: $Ba_{0.8}Sr_{0.2}TiO_3$ (single-domain without domain walls T_c 77 °C) and $Ba_{0.2}Sr_{0.8}TiO_3$ (no domain T_c – 148 °C).[15] The polar, nonpolar nature of the structures at room temperature has been confirmed by Raman, differential scanning calorimetry (DSC), microscopy, and XRD analysis. By measuring their photocatalytic decomposition of a dye molecule, we confirm that our nanoscale single crystalline single domain samples (without domain walls) still enhance the carrier separation with their inherent dipole. This proves that it is not necessary for a domain wall to be present for efficient carrier separation and that the dipole of the ferroelectric drives mobile carrier separation.

The phase composition of the as-produced samples was analyzed using XRD. The 20°–70° 2θ patterns obtained are shown in **Figure 1**a. The structure is single phase cubic. As expected, no obvious peak splitting was observed at $2\theta = 45°$ for $Ba_{0.8}Sr_{0.2}TiO_3$ in the tetragonal phase below the Curie point (T_c). This is believed to be related with the formation of the single domain single grain structures with decreased spontaneous distortion.[12] The transition at T_c from the cubic to the ferroelectric tetragonal structure is accompanied by spontaneous strain and a small volume increase. In micrometer sized grains which show single grain multidomain structures, the change of lattice dimensions and the internal stresses produced by the volume increase can be minimized by domain walls. In nanometer sized grains which show single grain single domain structures, domains walls are absent. Consequently, the resulting stresses cannot be relieved by domain walls. On average, the stresses are compressive because of the volume increase, thus tending to suppress the spontaneous distortion, which results in a reduced c/a ratio. This makes it difficult to distinguish between polar and nonpolar materials in an XRD pattern.[16]

The two BST samples have similar particles sizes measured using BET as shown in Table S1 (Supporting Information). The average particle size of $Ba_{0.8}Sr_{0.2}TiO_3$ was measured as 70.8 nm, for the $Ba_{0.2}Sr_{0.8}TiO_3$ sample it was 65.2 nm as measured from 100 particles imaged using SEM. The BET surface areas are 7.3904 $m^2\ g^{-1}$ for $Ba_{0.8}Sr_{0.2}TiO_3$ and 7.9646 $m^2\ g^{-1}$ for $Ba_{0.2}Sr_{0.8}TiO_3$ sample. The BET surface area represents a difference of 7% extra surface area for the nonpolar material. This material has the higher surface area but the lower photoactivity.

Further investigation of the microstructure of $Ba_{0.8}Sr_{0.2}TiO_3$ and $Ba_{0.2}Sr_{0.8}TiO_3$ was performed using TEM, shown in **Figure 2**. Analysis of the electron diffraction patterns (Figure 2b,e) for the nanoparticles identifies them as single crystals. It is noteworthy that the TEM generated diffraction

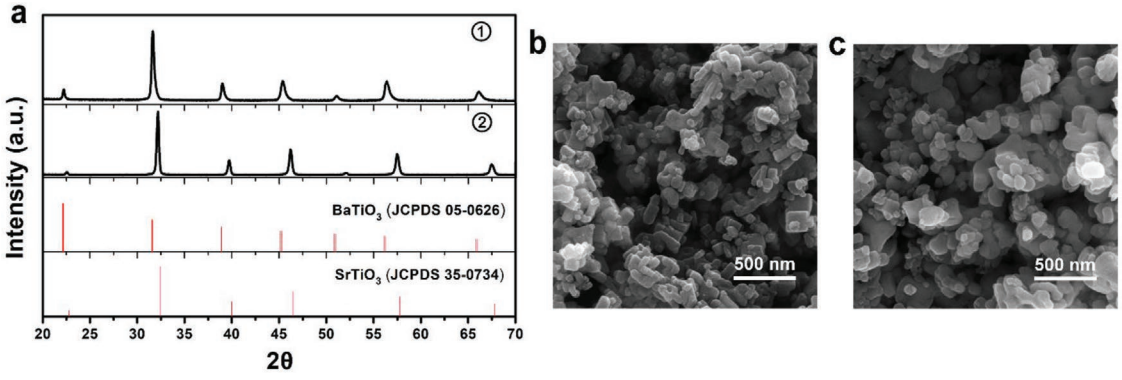

Figure 1. Phase and morphology of BST nanocrystals. a) X-ray diffraction (XRD) pattern of ① $Ba_{0.8}Sr_{0.2}TiO_3$ ② $Ba_{0.2}Sr_{0.8}TiO_3$. b) SEM micrograph of $Ba_{0.8}Sr_{0.2}TiO_3$ and c) SEM micrograph of $Ba_{0.2}Sr_{0.8}TiO_3$.

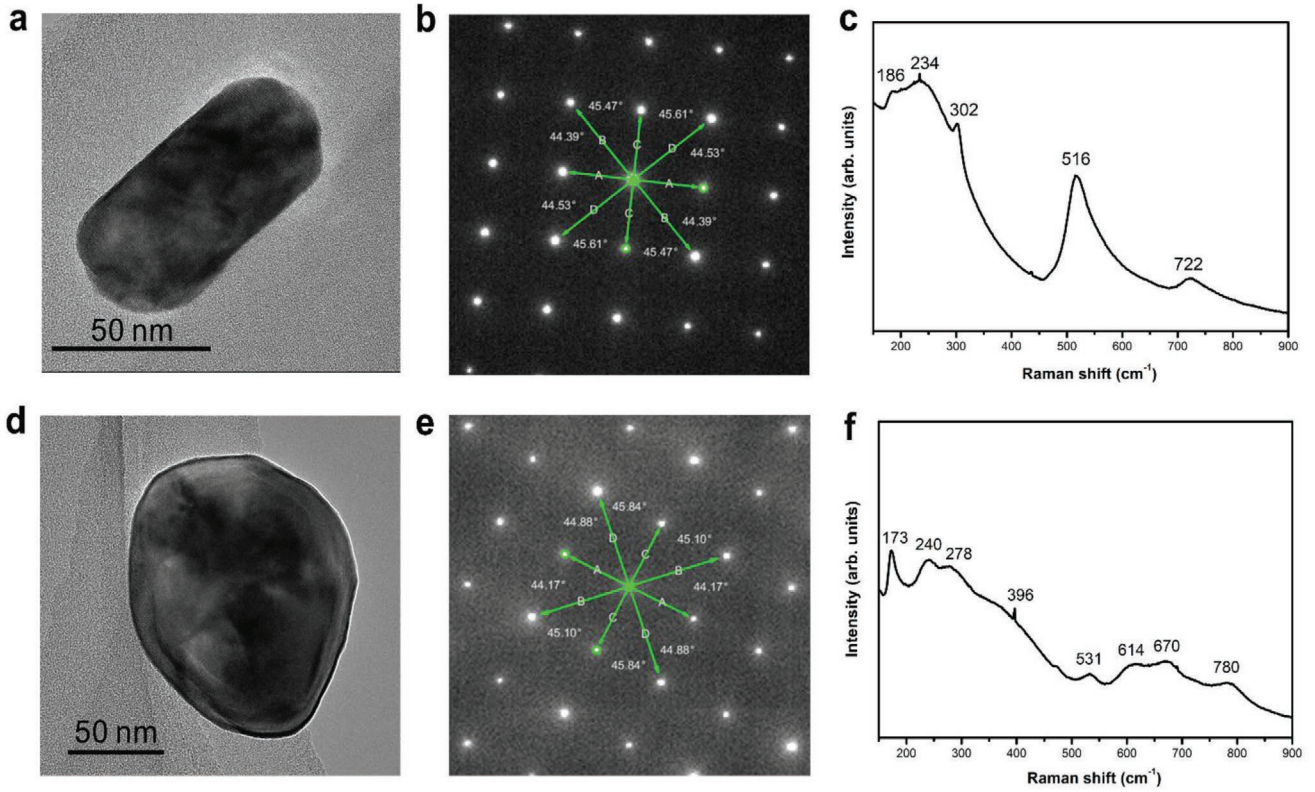

Figure 2. Microstructure and lattice dynamics characterization of BST. a,d) Transmission electron microscopy (TEM) image of a typical $Ba_{0.8}Sr_{0.2}TiO_3$ crystal and a $Ba_{0.2}Sr_{0.8}TiO_3$ crystal. b,e) Electron diffraction patterns of $Ba_{0.8}Sr_{0.2}TiO_3$ and $Ba_{0.2}Sr_{0.8}TiO_3$, respectively. c,f) Room-temperature Raman spectra of $Ba_{0.8}Sr_{0.2}TiO_3$ and $Ba_{0.2}Sr_{0.8}TiO_3$.

patterns also show a cubic structure for both samples. This is consistent with XRD results and suggests the requirement of suitable techniques to determine whether this nanoscale sample is polar or not. $Ba_{0.8}Sr_{0.2}TiO_3$, which is expected to have a spontaneous polarization, does not have any domain wall or other internal features in the TEM images. The single-domain structure of $Ba_{0.8}Sr_{0.2}TiO_3$ was further evidenced by the DSC measurements as detailed in Figure S1 (Supporting Information). The endothermic peak representing the tetragonal to cubic phase is not present in small-sized $Ba_{0.8}Sr_{0.2}TiO_3$ powders. The absence of this peak indicates that there has been a multi- to single-domain transformation in the sample.[12]

The high sensitivity of the Raman spectroscopy to short-range distortions such as microstructural defects and symmetry changes[12] makes it a suitable tool to study the polar nature of nanoscale ferroelectric materials. Raman spectra of $Ba_{0.8}Sr_{0.2}TiO_3$ and $Ba_{0.2}Sr_{0.8}TiO_3$ collected at room temperature are shown in Figure 2c,f. The characteristic peaks of ferroelectric order found in the spectrum of $Ba_{0.8}Sr_{0.2}TiO_3$ at 302 and 722 cm^{-1} indicate the tetragonal phase and polar nature of the sample. The peaks centered at 234 and 516 cm^{-1} have been attributed to disorder of titanium.[13] By contrast the spectrum for $Ba_{0.2}Sr_{0.8}TiO_3$ shows no peaks related to ferroelectric order. The Raman peaks found for $Ba_{0.2}Sr_{0.8}TiO_3$ are analogous to those reported for nanocrystalline $SrTiO_3$, a paraelectric materials lacking a ferroelectric response.[17] Temperature-dependent Raman spectra of the $Ba_{0.8}Sr_{0.2}TiO_3$ sample were obtained to reveal its phase transformation with temperature changing through the Curie point. The information is given in Figure S2 (Supporting Information). The two peaks at 302 and 722 cm^{-1} vanish when temperature increased from 25 to 200 °C, which further demonstrates polar nature of the sample.

Figure 3a shows optical properties of the $x = 0.2$ and 0.8 samples characterized by UV–vis diffuse reflectance spectroscopy. The band gaps of the samples have been estimated from the Tauc plot, shown in Figure 3b. The band gaps of $Ba_{0.8}Sr_{0.2}TiO_3$ and $Ba_{0.2}Sr_{0.8}TiO_3$ are both estimated to be 3.24 eV. This is to be expected as the Ti and O systems in the lattice most strongly influence the band gap and allow a comparison of the photoactivity based on similar light absorption characteristics. We, therefore, provide compelling evidence that we have produced two samples that differ substantially in their polar nature but are similar in other properties, such as band structure, surface area, and size (SEM and TEM data).

Figure 3c,d give the UV–vis absorption spectra of RhB dye solutions as a function of illumination time for the two photocatalysts. The maximum absorption peak for RhB was located at 554 nm with absorption by the dye, and it decreased with the illumination time. The absorbance at zero time at λ_{max} (554 nm) was taken as C_0. The concentrations of other samples, taken as C_i, are determined according to the absorption measurement at 540 nm where absorbance is proportional to the concentration. The percentage of photodecolorization X was calculated using Equation (1):

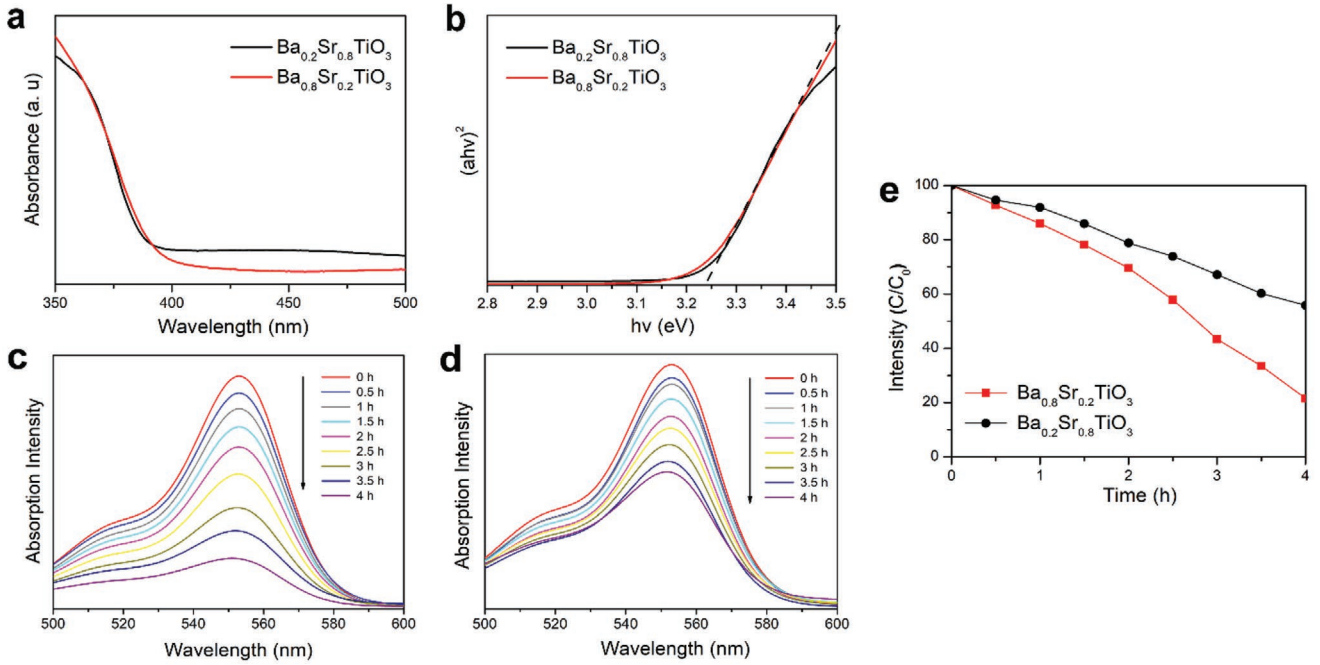

Figure 3. Optical property and photoactivity characterization of BST. a) UV–vis spectra of $Ba_{0.8}Sr_{0.2}TiO_3$ and $Ba_{0.2}Sr_{0.8}TiO_3$. b) Tauc plots of the nanocrystals derived from (a) to determine the optical band gaps. c,d) UV–vis absorption spectra of RhB dye solutions obtained at different degradation time with $Ba_{0.8}Sr_{0.2}TiO_3$ and $Ba_{0.2}Sr_{0.8}TiO_3$. e) Degradation of Rh B with the two catalysts under solar simulator to assess their photoactivity.

$$X(\%) = \left(1 - C_i / C_0\right) * 100 \quad (1)$$

The photodecolorization curves of RhB of the two $Ba_xSr_{1-x}TiO_3$ samples are shown in Figure 3e. It can be seen that $Ba_{0.8}Sr_{0.2}TiO_3$ shows an enhanced efficiency in RhB decolorization over $Ba_{0.2}Sr_{0.8}TiO_3$. The kinetics of photocatalytic decolorization of RhB follows the Langmuir–Hinshelwood model which can be simplified to a pseudo-first-order equation. Integration gives the relationship:[18]

$$\ln\left(\frac{C_i}{C_0}\right) = k_{obs}\, t \quad (2)$$

where k_{obs} is the reaction rate obtained from the slope of ln (C_0/C) versus t. The derived k_{obs} of the degradation process is shown in **Table 1**. A comparison of rate constants in Table 1 shows that the polar $Ba_{0.8}Sr_{0.2}TiO_3$ has a faster reaction rate than the nonpolar $Ba_{0.2}Sr_{0.8}TiO_3$. Our evaluation of the other physical properties (surface area and band gap) shows that these vary by less than k_{obs}. The two $Ba_xSr_{1-x}TiO_3$ materials possess close surface area and the same band gap values. Moreover, $Ba_{0.8}Sr_{0.2}TiO_3$ and $Ba_{0.2}Sr_{0.8}TiO_3$ are single grain single domain and nondomain structure, respectively. Our materials, therefore, allow for a comparison of spontaneous polarization effect without a contribution from domain walls. Thus, the enhanced photocatalytic performance of the $Ba_{0.8}Sr_{0.2}TiO_3$ can be attributed to the effect from its polar structure in the absence of domain walls. By the way, domain walls normally show low polarization values,[9] which suggest that the contribution of domain walls in terms of working as an electrical field to separate photo carriers (holes and electrons) is lower than that of domains.

Table 1. Obtained k_{obs} from the fitted linear plot of ln(C_0/C) versus t.

Dye solution concentration and volume	Catalyst	k_{obs} [min^{-1}]	R^2
10 mg L^{-1}, 50 ml	$Ba_{0.8}Sr_{0.2}TiO_3$, 0.15 g	0.1794	0.99
10 mg L^{-1}, 50 ml	$Ba_{0.2}Sr_{0.8}TiO_3$, 0.15 g	0.1147	0.97

Figure 4 provides a schematic of the energy level diagrams for the $Ba_xSr_{1-x}TiO_3$ samples. In $Ba_{0.8}Sr_{0.2}TiO_3$ which has the polar structure, band bending at the surface occurs due to the spontaneous polarization induced charge screening as that has been widely reported in ferroelectrics.[8,19] The spontaneous polarization P, pointing from the bounded negative charges to positive charges, creates an internal electric field which has the opposite direction to it and drives the free carriers within the material to two sides of the surface. Accumulation of these carriers causes upward and downward band bending at the surface respectively. This band bending situation happens in an ambient environment and is presented in Figure 4a. Compared to $Ba_{0.8}Sr_{0.2}TiO_3$, the nonpolar $Ba_{0.2}Sr_{0.8}TiO_3$ exhibits no internally driven band bending, as shown in Figure 4b. When the $Ba_xSr_{1-x}TiO_3$ samples contact an aqueous solution band bending occurs due to migration of mobile species across the semiconductor liquid interface,[20] the band bending situation is presented in Figure 4c,d. This process usually causes upward band bending for n type materials. The higher permittivity of polar structure is also useful to improve photocatalytic preference which is consistent with the work in bulk ceramics.[21] In the polar material, the polarization driven band bending enhances photocatalytic rate.

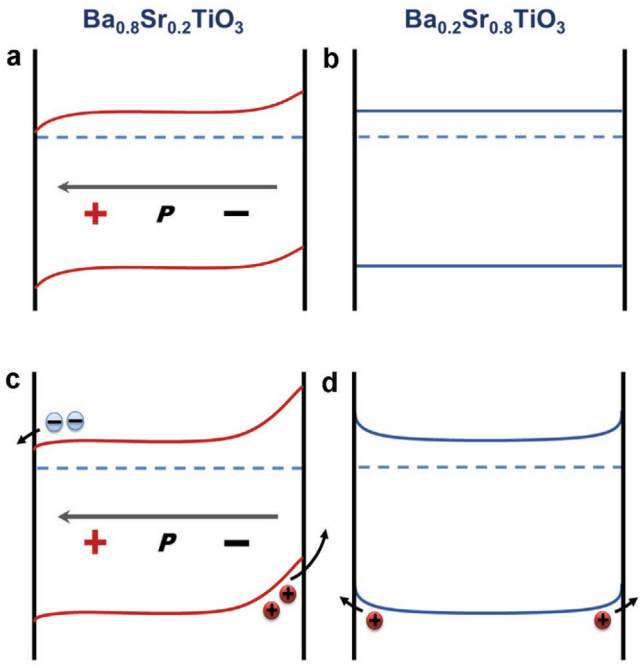

Figure 4. Schematic representation of the energy level diagrams for $Ba_{0.8}Sr_{0.2}TiO_3$ and $Ba_{0.2}Sr_{0.8}TiO_3$ in ambient (a,b) and aqueous solution (c,d). The polar $Ba_{0.8}Sr_{0.2}TiO_3$ has band bending in ambient condition due to the spontaneous polarization induced screening effect, with upward band bending occurs on the surface of C^- domain and downward band bending occurs on the surface of C^+ domain (a). The nonpolar $Ba_{0.2}Sr_{0.8}TiO_3$ in ambient condition has no band bending (b). When in contact with aqueous solution and energy equilibrium achieved, the upward band bending increases and downward band bending decreases in $Ba_{0.8}Sr_{0.2}TiO_3$ (c). $Ba_{0.2}Sr_{0.8}TiO_3$ behaves as a typical n type semiconductor and shows upward band bending in aqueous solution (d). ***P*** is the spontaneous polarization, which points from the negative charges to the positive charges.

2. Conclusions

In conclusion, we have produced nanometer sized $Ba_xSr_{1-x}TiO_3$ single crystals through a molten-salt method. The material $Ba_{0.8}Sr_{0.2}TiO_3$ exhibits a single crystal single domain morphology. The polar nature is dependent on the Currie point of the produced particles. Influence of polar nature on the photocatalytic activities of the nanoparticles was evaluated through photocatalytic mineralization of RhB. These results indicate that the decolorization rate was enhanced when the material with spontaneous polarization was used. We attribute this enhanced reaction rate to the separation of carriers due to the internal electric field present in polar structured ferroelectrics. Our results provide evidence that the internal electric field within a single domain can enhance carrier separation and increase photocatalytic activities.

Supporting Information

Supporting Information is available from the Wiley Online Library or from the author.

Acknowledgements

The authors would like to acknowledge the Chinese Scholarship Council for supporting this work. Financial supports from London South Bank University and the Wallenberg Academy Fellow Program (for Z. Z.) are acknowledged.

Conflict of Interest

The authors declare no conflict of interest.

Keywords

barium strontium titanates, domain wall free, ferroelectrics, photocatalysis

Received: May 31, 2020
Revised: July 11, 2020
Published online: August 12, 2020

[1] M. R. Morris, S. R. Pendlebury, J. Hong, S. Dunn, J. R. Durrant, *Adv. Mater.* **2016**, *28*, 7123.
[2] S. Li, J. Eastman, Z. Li, C. Foster, R. Newnham, L. Cross, *Phys. Lett. A* **1996**, *212*, 341.
[3] A. Kakekhani, S. Ismail-Beigi, *J. Mater. Chem. A* **2016**, *4*, 5235.
[4] a) L. Pan, S. Sun, Y. Chen, P. Wang, J. Wang, X. Zhang, J.-J. Zou, Z. L. Wang, *Adv. Energy Mater.* **2020**, *10*, 2000214; b) J. Chen, H. Lu, H.-J. Liu, Y.-H. Chu, S. Dunn, K. Ostrikov, A. Gruverman, N. Valanoor, *Appl. Phys. Lett.* **2013**, *102*, 182904; c) Y. Cui, S. M. Goldup, S. Dunn, *RSC Adv.* **2015**, *5*, 30372; d) N. V. Burbure, P. A. Salvador, G. S. Rohrer, *Chem. Mater.* **2010**, *22*, 5831.
[5] a) M. Ahmadi, L. Collins, A. Puretzky, J. Zhang, J. K. Keum, W. Lu, I. Ivanov, S. V. Kalinin, B. Hu, *Adv. Mater.* **2018**, *30*, 1705298; b) D. Kim, J. S. Yun, P. Sharma, J. Kim, A. M. Soufiani, S. Huang, M. A. Green, A. W. Ho-Baillie, J. Seidel, *Nat. Commun.* **2019**, *10*, 444.
[6] a) H. Röhm, T. Leonhard, M. J. Hoffmann, A. Colsmann, *Energy Environ. Sci.* **2017**, *10*, 950; b) K. Miyata, X.-Y. Zhu, *Nat. Mater.* **2018**, *17*, 379.
[7] D. Meggiolaro, F. Ambrosio, E. Mosconi, A. Mahata, F. De Angelis, *Adv. Energy Mater.* **2020**, *10*, 1902748.
[8] S. V. Kalinin, D. A. Bonnell, T. Alvarez, X. Lei, Z. Hu, J. Ferris, Q. Zhang, S. Dunn, *Nano Lett.* **2002**, *2*, 589.
[9] G. Nataf, M. Guennou, J. Kreisel, P. Hicher, R. Haumont, O. Aktas, E. Salje, L. Tortech, C. Mathieu, D. Martinotti, *Phys. Rev. Mater.* **2017**, *1*, 074410.
[10] B. I. Sturman, V. M. Fridkin, *The Photovoltaic and Photorefractive Effects in Noncentrosymmetric Materials*, Vol. *8*, Gordon and Breach, London **1992**.
[11] a) C.-L. Jia, S.-B. Mi, K. Urban, I. Vrejoiu, M. Alexe, D. Hesse, *Nat. Mater.* **2008**, *7*, 57;. b) C. T. Nelson, B. Winchester, Y. Zhang, S.-J. Kim, A. Melville, C. Adamo, C. M. Folkman, S.-H. Baek, C.-B. Eom, D. G. Schlom, L.-Q. Chen, X. Pan, *Nano Lett.* **2011**, *11*, 828.
[12] M. H. Frey, D. A. Payne, *Phys. Rev. B* **1996**, *54*, 3158.
[13] M. B. Smith, K. Page, T. Siegrist, P. L. Redmond, E. C. Walter, R. Seshadri, L. E. Brus, M. L. Steigerwald, *J. Am. Chem. Soc.* **2008**, *130*, 6955.

[14] M. J. Polking, M.-G. Han, A. Yourdkhani, V. Petkov, C. F. Kisielowski, V. V. Volkov, Y. Zhu, G. Caruntu, A. Paul Alivisatos, R. Ramesh, *Nat. Mater.* **2012**, *11*, 700.
[15] a) L. Zhou, P. Vilarinho, J. Baptista, *J. Eur. Ceram. Soc.* **1999**, *19*, 2015; b) J. Nowotny, M. Rekas, *Key Eng. Mater.* **1992**, *66–67*, 45.
[16] Z. Zhao, V. Buscaglia, M. Viviani, M. T. Buscaglia, L. Mitoseriu, A. Testino, M. Nygren, M. Johnsson, P. Nanni, *Phys. Rev. B* **2004**, *70*, 024107.
[17] F. A. Rabuffetti, H.-S. Kim, J. A. Enterkin, Y. Wang, C. H. Lanier, L. D. Marks, K. R. Poeppelmeier, P. C. Stair, *Chem. Mater.* **2008**, *20*, 5628.
[18] J.-M. Herrmann, *Catal. Today* **1999**, *53*, 115.
[19] S. Dunn, P. M. Jones, D. E. Gallardo, *J. Am. Chem. Soc.* **2007**, *129*, 8724.
[20] L. Li, P. A. Salvador, G. S. Rohrer, *Nanoscale* **2014**, *6*, 24.
[21] A. Bhardwaj, N. V. Burbure, G. S. Rohrer, *J. Am. Ceram. Soc.* **2010**, *93*, 4129.